

OPEN

Retinopathy of Prematurity and Bronchopulmonary Dysplasia are Independent Antecedents of Cortical Maturation Abnormalities in Very Preterm Infants

Julia E. Kline¹, Venkata Sita Priyanka Illapani¹, Lili He^{1,2}, Mekibib Altaye^{2,4} & Nehal A. Parikh^{1,2,3*}

Very preterm (VPT) infants are at high-risk for neurodevelopmental impairments, however there are few validated biomarkers at term-equivalent age that accurately measure abnormal brain development and predict future impairments. Our objectives were to quantify and contrast cortical features between full-term and VPT infants at term and to associate two key antecedent risk factors, bronchopulmonary dysplasia (BPD) and retinopathy of prematurity (ROP), with cortical maturational changes in VPT infants. We prospectively enrolled a population-based cohort of 110 VPT infants (gestational age ≤ 31 weeks) and 51 healthy full-term infants (gestational age 38–42 weeks). Structural brain MRI was performed at term. 94 VPT infants and 46 full-term infants with high-quality T2-weighted MRI were analyzed. As compared to full-term infants, VPT infants exhibited significant global cortical maturational abnormalities, including reduced surface area (–5.9%) and gyrification (–6.7%) and increased curvature (5.9%). In multivariable regression controlled for important covariates, BPD was significantly negatively correlated with lobar and global cortical surface area and ROP was significantly negatively correlated with lobar and global sulcal depth in VPT infants. Our cohort of VPT infants exhibited widespread cortical maturation abnormalities by term-equivalent age that were in part anteceded by two of the most potent neonatal diseases, BPD and ROP.

Worldwide, preterm birth affects slightly over 10% of pregnancies¹. Although the survival rate has increased dramatically, preterm-born infants remain at high risk for neurodevelopmental impairments (NDI). Infants born very preterm, at less than 31 weeks gestational age (GA), often develop NDI such as cognitive, behavioral, and psychological abnormalities^{2–4}. Many also develop motor impairments, including the 10% who develop cerebral palsy⁵.

On structural magnetic resonance imaging (MRI) at term-equivalent age (TEA), preterm infants exhibit white matter signal abnormalities, destructive abnormalities, and global and regional brain tissue volume decreases that are associated with NDI^{6–8}. Changes in cortical maturational features may also be early biomarkers of NDI. Premature infants have less cortical surface area than full term controls⁹, which is correlated with diminished cognitive ability later in life^{10–12}. Preterm infants also have altered cortical folding, which can be assessed via a number of metrics. For instance, gyrification index, or the ratio of cortex within the sulcal folds to cortex on the outer brain surface, is decreased in preterm infants compared to term controls^{13,14}. A complementary folding metric, sulcal depth, tends to primarily decrease^{13–15} in preterm groups. Curvature of the inner cortical surface/outer white matter is also reportedly increased in preterm infants¹⁶. Given that a significant amount of cortical expansion and folding occurs in the third trimester¹⁷, these alterations are likely caused by early exposure to the ex-utero environment^{16,18} and the secondary illnesses and interventions that premature babies are at risk for^{13,19}.

¹Perinatal Institute, Cincinnati Children's Hospital Medical Center, Cincinnati, OH, USA. ²Department of Pediatrics, University of Cincinnati College of Medicine, Cincinnati, OH, USA. ³Center for Perinatal Research, The Research Institute at Nationwide Children's Hospital, Columbus, OH, USA. ⁴Division of Biostatistics, Cincinnati Children's Hospital Medical Center, Cincinnati, OH, USA. *email: Nehal.Parikh@cchmc.org

One such secondary illness, bronchopulmonary dysplasia (BPD) is a chronic lung disease that affects mostly preterm-born infants who require prolonged mechanical ventilation or continuous positive airway pressure and supplementary oxygen for respiratory distress syndrome²⁰. BPD has been linked to adverse neurodevelopmental outcomes such as cerebral palsy²¹, cognitive deficits²², language deficits^{23,24}, and many combinations thereof^{25–27}. Another secondary illness, retinopathy of prematurity (ROP) is a potentially blinding eye disease, which is also found predominantly in premature infants and has been linked to the overuse of oxygen and early illness severity. It has been suggested that ROP is more than just an eye disease and is related to pathology of both the retina and the neurovasculature²⁸. Severe ROP is associated with delayed white matter maturation, poorer cognitive and motor scores at 18 months²⁹ and lower IQ in adolescence³⁰. There is evidence that BPD and ROP tend to co-occur, but they are independently predictive of neurodevelopmental impairment²⁷. For instance, in a large population-based study, the combination of BPD, ROP, and brain injury, strongly and independently predicted the risk of disability in very low birth weight infants³¹. However, no prior studies have linked these two common preterm morbidities with abnormal cortical features at TEA.

Our objectives were: (1) quantify and contrast cortical features between full-term (FT) and very preterm (VPT) infants in 50 brain regions in a large population-based cohort and (2) examine the impact of two of the most potent neonatal diseases, ROP and BPD, on these cortical features, while controlling for known covariates. We hypothesized that (1) preterm infants would show widespread significant alterations in cortical features compared to the full-term control group, namely decreased cortical surface area, gyrification, and sulcal depth and increased white matter curvature and (2) BPD and ROP would be correlated with the objectively-quantified cortical features in the preterm group. These analyses should (1) objectively quantify early alterations in cortical features in premature infants, which may serve as early biomarkers of NDI and (2) shed light on specific secondary illnesses which may exacerbate these alterations.

Methods

Subjects. We prospectively enrolled 110 VPT infants from four level III NICUs from December 2014 to April 2016. These NICUs – Nationwide Children’s Hospital, Ohio State University Medical Center, Riverside Hospital, and Mount Carmel St. Ann’s Hospital – cared for approximately 80% of VPT births in the Columbus, Ohio region. We prospectively enrolled 51 healthy FT control infants from September 2014 to August 2015 from the well-baby nurseries of these hospitals. The inclusion criteria for full term infants included a GA of 38–42 weeks, appropriate weight for GA, and a normal well-baby nursery course. Full-term exclusions included congenital/chromosomal anomalies of the brain, spine, heart, or lungs, significant maternal conditions (e.g. insulin-dependent diabetes or severe preeclampsia), intrauterine drug or alcohol exposure, and a history of perinatal distress or complications. Preterm inclusion criteria included a GA of ≤ 31 weeks, while exclusion criteria included congenital/chromosomal anomalies of the brain, spine, or heart (e.g. Dandy-Walker malformation, myelomeningocele, cyanotic heart disease). We excluded any infants hospitalized at 44 weeks postmenstrual age (unless they were at Nationwide Children’s Hospital, the site of imaging). The Nationwide Children’s Hospital Institutional Review Board approved the study (Protocol#: IRB13-00636). Reciprocity agreements with the Institutional Review Boards of Nationwide Children’s Hospital, Ohio State University Medical Center, Riverside Hospital, and Mount Carmel St. Ann’s Hospital allowed for approval at all sites. The study methods were carried out in accordance with the relevant guidelines and regulations. Written informed consent was obtained from a parent or guardian of all infants.

Imaging methods. MRI data was acquired on a 3T Siemens Skyra scanner at Nationwide Children’s Hospital at a mean (SD) postmenstrual age of 40.2 (0.6) weeks for the VPT cohort and 41.3 (0.8) weeks for the FT cohort. The majority of infants at Nationwide were imaged while inpatients, and all infants from the other NICUs were imaged after discharge. The scans were overseen by a skilled neonatal nurse and a neonatologist, who monitored heart rate and oxygen saturations throughout. We performed imaging without sedation using these procedures: the infant was fed 30 minutes prior to MRI, silicone earplugs were placed (Instaputty, E.A.R. Inc, Boulder, CO), and a blanket and vacuum immobilization device (MedVac, CFI Medical Solutions, Fenton, MI) helped promote natural sleep. We used these acquisition parameters: axial T2-weighted: echo time 147 ms, repetition time 9500 ms, flip angle 150°, resolution $0.93 \times 0.93 \times 1.0$ mm³, scan time 4:09 min. Additional sequences such as T1- and susceptibility-weighted images were acquired for qualitative assessment of abnormality.

MRI processing. All T2-weighted images were postprocessed using the developing Human Connectome Pipeline (dHCP)³² developed for neonatal MRI, in order to automatically extract global and regional values for cortical features. The dHCP pipeline leverages FreeSurfer for tissue segmentation and volume estimation. It also calculates a value for the cortical features of interest, surface area, gyrification index, sulcal depth, and inner cortical curvature, for each of the 50 regions of the Gousias neonatal atlas³³ and for the whole brain. All tissue segmentations (Fig. 1) and cortical surface results were visually inspected. Any scan with significant movement artifact, missing cortical boundaries, or moderate to severe ventriculomegaly was excluded at this point, as ventriculomegaly tended to interfere with proper tissue classification by the dHCP.

Statistical analysis. Our first major statistical analysis assessed significant differences in global and regional cortical features between the full-term and the very preterm groups. We began by transforming non-normal cortical feature values using either log transforms, power transforms, or the Yeo-Johnson transform³⁴ (for negative values), as appropriate. We then applied analysis of covariance (ANCOVA) to calculate significant group differences in the global and regional cortical features. We performed the ANCOVA analysis two ways: 1) with postmenstrual age (PMA) at MRI as the only covariate and 2) with PMA at MRI and total tissue volume (TTV) both as covariates. TTV was included to correct for the difference in brain size between the very preterm and

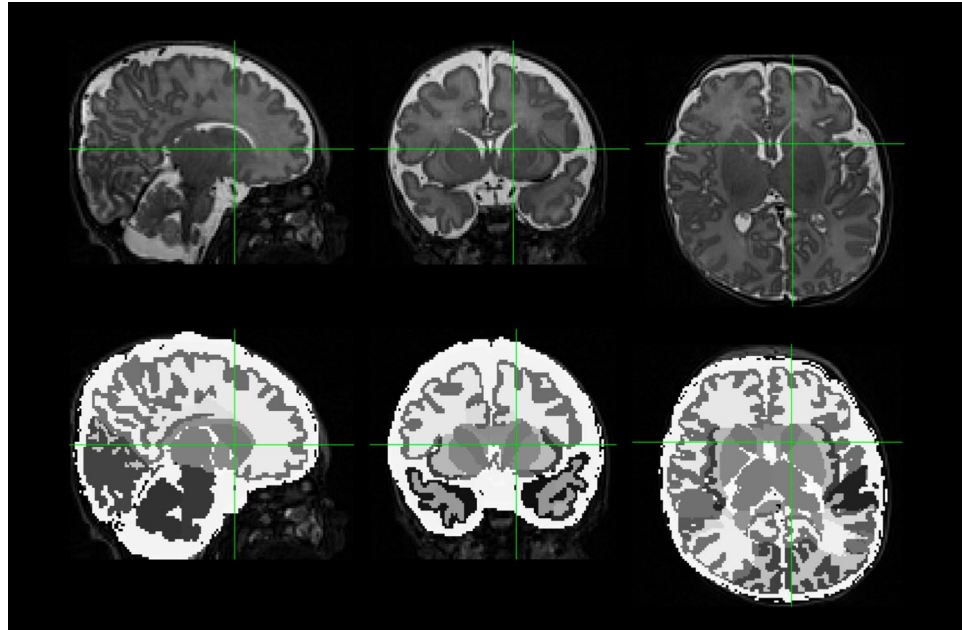


Figure 1. An example T2-weighted MRI scan from one VPT subject is shown in sagittal, coronal, and horizontal views (top row). A segmentation from the Developing Human Connectome Pipeline (dHCP) is overlaid on the original image (bottom row). The dHCP performs cortical and sub-cortical volume segmentation, cortical surface extraction, and cortical surface inflation and was specifically designed for neonatal T2-weighted MRI brain scans.

the full term infants^{35–37}. We did not use total cranial volume as a covariate in any analyses, because the very preterm group had significantly increased ventricular volume, despite the exclusion of subjects with ventriculomegaly. Following the ANCOVA, we used the ‘adjust’ command in Stata to center the covariates on their means and obtain the adjusted group means, which were then transformed back to their original units, if applicable. Because we analyzed so many cortical metrics (>200), we corrected for false discovery rate (FDR) using the Benjamini-Hochberg procedure with a chosen false discovery rate of 5%.

Our second major statistical analysis was a multivariable linear regression analysis examining the impact of BPD and ROP on all four global cortical metrics in the very preterm group, adjusted for covariates. We defined BPD (any severity) per Jobe and Bancalari’s original definition³⁸ and ROP using the International Classification of ROP guidelines³⁹. Because we hypothesized that BPD and ROP would predict cortical metric values independently of other known clinical or social demographic covariates, we took care to determine the best covariates for each regression. For each regression/global cortical metric, we started with 20 possible covariates (Table 1) from three distinct time periods – the antenatal, intrapartum, and postnatal periods – that had been associated with BPD, ROP, or NDI in previous research. We performed a sequential covariate selection method that has been published on several times previously^{37,40,41}. Potential covariates were first tested with only other potential covariates from the same time period. For each individual period, covariates correlated with the cortical metric of interest at $p < 0.25$ were all entered into backward stepwise regression⁴², and were deemed significant for that period if $p < 0.05$ in multi-variable regression. Covariates deemed significant from all periods using the above criteria were included in the final model, even if they became non-significant with the addition of other covariates. Overall, this method 1) prevents later-occurring significant covariates from displacing earlier-occurring significant covariates and 2) helps avoid overfitting the model with too many covariates. Known highly-important covariates of brain development, PMA at MRI and injury score on structural MRI⁴³, were forced into all final models. Next, we fit all resultant cortical surface metric models for each individual lobe, using multivariate regression in Stata, to determine whether the associations between BPD/ROP and cortical surface metrics were strongly regional.

Finally, we performed a third minor statistical analysis, using Pearson correlation analysis to assess the interrelation between all four global cortical metrics. All analyses were performed in STATA 15.1 (Stata Corp., College Station, TX), except the Benjamini-Hochberg analysis, which was performed in python.

Results

Of the 110 eligible VPT infants, one was missing a T2 image, 10 had significant ventriculomegaly that adversely affected brain segmentation. Four T2 images had significant artifact, and one had missing cortical boundaries. The remaining 94 infants were included in the analysis. Of these, only one infant had significant macrostructural injury on MRI. Of the 51 eligible FT subjects, four T2 images had missing boundaries, and one had poor alignment with the dHCP atlas. The remaining 46 were included in the analysis. Table 1 shows the baseline characteristics of our cohorts.

Characteristics	Very Preterm Infants (N = 94)
Antenatal	
Chorioamnionitis, n (%)	14 (14.9)
Antenatal steroids, n (%)	82 (87.2)
Male, n (%)	53 (56.4)
Intrauterine growth restriction	7 (7.4)
Intrapartum	
Gestational age (weeks), mean (SD)	28.3 (2.5)
Birth weight (g), mean (SD)	1121.7 (394.1)
Head circumference (mm), mean (SD)	25.6 (3.0)
Low NICU admission temperature, n (%)	27 (28.7)
Apgar score at 5 minutes <5, n (%)	18 (19.4)
Postpartum/neonatal	
Total parenteral nutrition (days), mean (SD)	18.9 (18.0)
Days of maternal breast milk in first 28 days, mean (SD)	23.5 (6.8)
Late onset culture-positive sepsis, n (%)	13 (13.8)
Patent ductus arteriosus, n (%)	20 (21.3)
Necrotizing enterocolitis, n (%)	10 (10.6)
Caffeine treatment, n (%)	83 (88.3)
Moderate or severe injury on structural MRI, n (%)	9 (9.6)
Surgery for necrotizing enterocolitis and spontaneous intestinal perforation, n (%)	5 (5.3)
Major surgery during NICU stay, n (%)	13 (13.8)
Moderate or severe bronchopulmonary dysplasia, n (%)	48 (51.1)
Retinopathy of prematurity, n (%)	46 (48.9)
Post menstrual age at scan, mean (SD), range	40.2 (0.6), (39.3–43.1)
Full-Term Infants (N = 46)	
Male, n (%)	22 (47.8)
Gestational age (weeks), mean (SD)	39.5 (0.8)
Post menstrual age at scan, mean (SD), range	41.3 (0.8), (40.0–43.0)

Table 1. Characteristics of the final very preterm and full-term cohorts.

The results of our two ANCOVA group analyses were highly similar; therefore, we will present results controlled for both PMA at MRI and TTV. (Results controlled for PMA only are in the supplement.) Globally, compared to the full-term infants, the very preterm infants showed a 6 to 7% reduction in both surface area and gyrification index and a 6% increase in curvature. Whole-brain sulcal depth was not significantly different between the groups (Table 2).

Regionally, the very preterm cohort had reduced surface area bilaterally in the frontal, parietal, and temporal lobes and in the insula and the right occipital lobe compared to the full-term group. (Range: 3.1% to 9.0%). VPT surface area increased (13.5%) only in the left fusiform gyrus (Fig. 2A). The VPT infants had reduced gyrification in bilateral regions of all lobes (Range: 6.1% to 24.0%.) compared to the full-term group, with the largest decreases in the temporal lobes. (Fig. 2B). Very preterm curvature increased in bilateral regions of the frontal, parietal, and temporal lobes (7.1% to 85.7%.) compared to the full-term group, with extreme values in the bilateral fusiform gyrus (586.0% right; 238.6% left) (Fig. 2C), however given the small size of this structure, its magnitude may be spurious. Curvature decreased in only one region in the VPT group, the bilateral parahippocampal gyrus (16.5% right; 13.8% left). Although there was no significant difference between groups for global sulcal depth, our preterm group had many significant regional sulcal depth differences compared to the full-term group (Fig. 2D) in the frontal, parietal, and temporal lobes. (Range: –100.4% to 41.5%).

Our preterm only regression analysis uncovered correlations between BPD and surface area and ROP and sulcal depth, in bivariable analysis and in multivariable regression adjusted for covariates. For surface area, the significant clinical covariates from the sequential variable selection procedure^{37,40,41} were injury score on MRI, PMA at MRI, sex, intrauterine growth restriction, head circumference at birth, and maternal breastmilk duration within the first 28 postnatal days. In a multivariable model with these covariates, BPD was negatively correlated with surface area ($p = 0.009$) (Table 3). The significant clinical covariates chosen for sulcal depth were injury score on MRI, PMA at MRI, GA, and birth weight z-score. In a multivariable model with these covariates, ROP was negatively correlated with sulcal depth ($p = 0.032$) (Table 3). ROP was not significantly correlated with surface area and BPD was not significantly correlated with sulcal depth in multi-variable regression with covariates. Likewise, BPD and ROP were both not significantly correlated with either gyrification index or curvature in multi-variable regression with covariates. Regionally, BPD was significantly negatively correlated with surface area in all lobes of the brain (Table 4). ROP was significantly negatively correlated with sulcal depth in the parietal lobe (Table 5).

Surface Metrics	Very Preterm Infants (N = 94)	Full-term Infants (N = 46)	Relative Percent Difference, Mean (95% CI)	P
Gyrification Index (unitless)	2.49 (0.20)	2.67 (0.30)	-6.74% (-9.90%, -3.58%)	<0.001
Surface Area (mm ²)	81210.10 (4527.51)	86252.30 (6836.50)	-5.85% (-8.07%, -3.62%)	<0.001
Curvature (1/mm)	2.14 (0.25)	2.02 (0.38)	5.94% (0.68%, 11.20%)	0.002
Sulcal Depth (unitless; mean convexity/concavity)	24.54 (3.42)	24.66 (5.16)	-0.49% (-5.39%, 6.36%)	0.84

Table 2. Whole-brain mean values and percent differences for four global cortical metrics in very preterm and full-term infants (corrected for PMA at MRI scan and TTV).

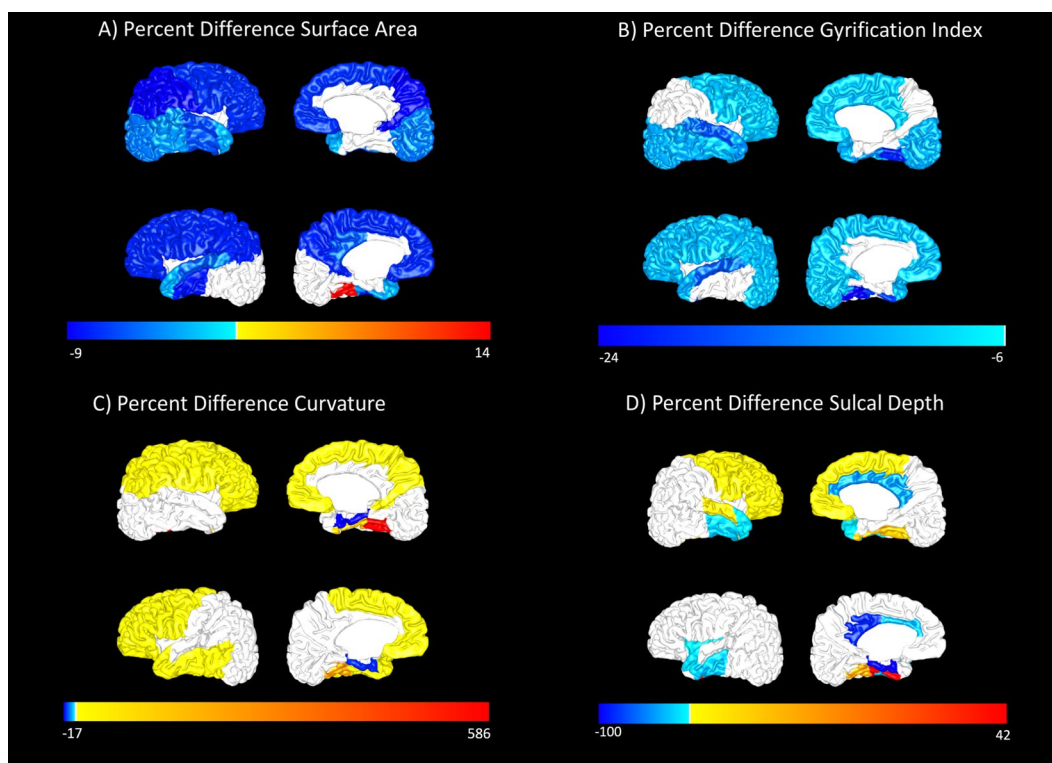


Figure 2. Mean Percent Difference in Cortical Metrics (Full-term to Very Preterm). Regional percent differences in adjusted group means for surface area (panel A), gyrification index (panel B), curvature of the white matter surface (panel C), and sulcal depth (panel D). For regions with significant differences between groups (after false discovery rate correction), percent difference values $(VPT - FT)/FT * 100$ are projected onto a representative subject brain from the very preterm group. These values have been corrected for postmenstrual age at MRI scan and total brain tissue volume. For each panel, Top row: right hemisphere; Bottom row: left hemisphere.

Our four global cortical metrics were strongly and significantly interrelated. Sulcal depth had a significant negative relationship with curvature ($r = -0.37$) and a positive relationship with surface area ($r = 0.34$). Curvature was significantly negatively correlated with both gyrification index ($r = -0.20$) and surface area ($r = -0.40$). Gyrification index was positively correlated with surface area ($r = 0.28$). Sulcal depth and gyrification index were not significantly correlated.

Discussion

Our results extend published findings of significant cortical maturation abnormalities in very preterm infants at TEA. Overall, our very preterm group showed decreased global and regional gyrification, decreased global and regional surface area, and increased global and regional curvature compared to the full-term group. Our preterm group also showed regional alterations in sulcal depth compared to the full-term group, with decreases tending to dominate. Unlike prior studies, we also identified two important risk factors – BPD and ROP – for abnormal changes in surface area and sulcal depth, respectively. In prior neuroimaging studies, preterm infants with BPD

Clinical Risk Factors	Multivariable regression	P value
	Coefficients (95% CI)	
Surface Area		
Male Sex	6626.74 (3444.97, 9808.51)	<0.001
Intrauterine growth restriction	-8773.05 (-14955.95, -2590.14)	0.006
Head circumference at birth	453.60 (-246.23, 1153.43)	0.201
Maternal breast milk duration (days)	327.29 (86.98, 567.61)	0.008
Postmenstrual age	3621.56 (1023.68, 6219.43)	0.007
Injury score on structural MRI	133.81 (-697.31, 964.94)	0.750
Bronchopulmonary dysplasia	-5508.80 (-9603.97, -1413.64)	0.009
Sulcal Depth		
Gestational age	0.36 (0.09, 0.62)	0.009
Z-score of birth weight	0.49 (-0.19, 1.17)	0.154
Postmenstrual age	0.37 (-0.44, 1.18)	0.364
Injury score on structural MRI	0.13 (-0.14, 0.40)	0.348
Retinopathy of prematurity	-1.44 (-2.76, -0.13)	0.032

Table 3. Multivariable Regression Models of Cortical Surface Area and Sulcal Depth.

	Coefficients (95% CI)	P value
Occipital Lobe Surface Area		
Male Sex	384.60 (56.20, 713.00)	0.022
Intrauterine growth restriction	-916.76 (-1554.92, -278.60)	0.005
Head circumference at birth	10.12 (-62.11, 82.35)	0.781
Maternal breast milk duration (days)	29.09743 (4.29, 53.90)	0.022
Postmenstrual age	118.36 (-149.78, 386.49)	0.383
Injury score on structural MRI	5.72 (-80.06, 91.51)	0.895
Bronchopulmonary dysplasia	-548.98 (-971.65, -126.30)	0.012
Parietal Lobe Surface Area		
Male Sex	658.36 (285.90, 1030.82)	0.001
Intrauterine growth restriction	-952.96 (-1676.74, -229.19)	0.010
Head circumference at birth	80.90 (-1.03, 162.82)	0.053
Maternal breast milk duration (days)	38.83 (10.69, 66.96)	0.007
Postmenstrual age	505.56 (201.45, 809.67)	0.001
Injury score on structural MRI	-11.61 (-108.90, 85.68)	0.813
Bronchopulmonary dysplasia	-532.13 (-1011.52, -52.75)	0.030
Temporal Lobe Surface Area		
Male Sex	660.71 (320.71, 1000.71)	<0.001
Intrauterine growth restriction	-791.03 (-1451.72, -130.34)	0.020
Head circumference at birth	36.14 (-38.64, 110.92)	0.339
Maternal breast milk duration (days)	35.21 (9.53, 60.89)	0.008
Postmenstrual age	403.11 (125.51, 680.71)	0.005
Injury score on structural MRI	58.78 (-30.03, 147.59)	0.192
Bronchopulmonary dysplasia	-573.45 (-1011.05, -135.86)	0.011
Frontal Lobe Surface Area		
Male Sex	1307.21 (740.90, 1873.52)	<0.001
Intrauterine growth restriction	-1399.86 (-2500.33, -299.39)	0.013
Head circumference at birth	86.16 (-38.40, 210.72)	0.173
Maternal breast milk duration (days)	50.82 (8.04, 93.59)	0.020
Postmenstrual age	635.40 (173.01, 1097.78)	0.008
Injury score on structural MRI	17.56 (-130.37, 165.49)	0.814
Bronchopulmonary dysplasia	-906.57 (-1635.45, -177.69)	0.015

Table 4. Multivariate regression associating BPD with surface area for each individual lobe, after controlling for important covariates.

	Coefficients (95% CI)	P value
Occipital Lobe Sulcal Depth		
Gestational age	1.16 (0.15, 2.16)	0.024
Z-score of birth weight	2.33 (−0.23, 4.89)	0.074
Post menstrual age	2.30 (−0.75, 5.36)	0.138
Injury score on structural MRI	0.17 (−0.85, 1.19)	0.740
Retinopathy of prematurity	3.36 (−1.61, 8.33)	0.183
Parietal Lobe Sulcal Depth		
Gestational age	0.68 (0.09, 1.28)	0.024
Z-score of birth weight	−0.19 (−1.70, 1.32)	0.805
Post menstrual age	1.06 (−0.74, 2.86)	0.246
Injury score on structural MRI	0.07 (−0.54, 0.67)	0.830
Retinopathy of prematurity	−3.39 (−6.32, −0.46)	0.024
Temporal Lobe Sulcal Depth		
Gestational age	−0.01 (−0.69, 0.68)	0.981
Z-score of birth weight	0.41 (−1.33, 2.16)	0.639
Post menstrual age	−0.49 (−2.57, 1.59)	0.640
Injury score on structural MRI	0.08 (−0.62, 0.78)	0.824
Retinopathy of prematurity	−0.53 (−3.91, 2.86)	0.758
Frontal Lobe Sulcal Depth		
Gestational age	0.41 (−0.15, 0.96)	0.148
Z-score of birth weight	0.18 (−1.23, 1.59)	0.798
Post menstrual age	−0.05 (−1.73, 1.63)	0.953
Injury score on structural MRI	0.12 (−0.44, 0.69)	0.664
Retinopathy of prematurity	−2.48 (−5.22, 0.26)	0.075

Table 5. Multivariate regression associating ROP with sulcal depth for each individual lobe, after controlling for important covariates.

and ROP have not exhibited consistent structural abnormalities to suggest that ROP and BPD-associated NDI are mediated through qualitative abnormalities visible on structural MRI. Although we cannot determine a definitive causal link, our results suggest that aberrant cortical maturation could be in the causal pathway between severe neonatal illnesses like ROP and BPD and future NDI.

Reduced surface area in preterm subjects is well-documented at TEA^{10,13} and in childhood^{11,12}, and reduced gyrification index in preterm subjects is also well-documented at TEA^{13,14,44}. Engelhardt *et al.* reported approximately 13% reduced gyrification and 19% reduced surface area in preterm infants compared to full-term infants at TEA, which is larger than our finding (7% reduced gyrification and 6% reduced surface area, globally). However, we excluded subjects with ventriculomegaly or injuries such as intraventricular hemorrhage (27% of the preterm subjects in Engelhardt's study had intraventricular hemorrhage), and we studied twice as many infants. Zhang reported 4% reduced gyrification index and 10% reduced cortical surface area in preterm children at seven years of age, which is closer to our result, albeit in a different age group. Zhang normalized their gyrification and surface area measures by convex hull area and total cortical surface area, respectively, while Engelhardt reported unnormalized group differences. Both normalization methods are fundamentally different from our analysis, in which we corrected for PMA at MRI and TTV. The differences in magnitude between our study and these previous studies can likely be explained by the injury status of the preterm cohort and the type of normalization performed.

Other works examining sulcal depth in very preterm subjects have reported just decreases¹⁴ or both increases and decreases at TEA¹³ and in childhood¹⁵, with decreases tending to dominate. Although there was no global difference between our two groups, there were more significant regional sulcal depth decreases (12) than increases (five) in the very preterm group, which is consistent with previous work.

Curvature was increased at TEA in our VPT group, which corroborates Makropoulos *et al.*'s findings¹⁶. Many different curvature formulations have been utilized, making this a challenging metric to compare to previous work. Curvature has been reported on both the outer cortical surface and on the inner cortical/outer white matter surface, as in the current work. It has been formulated as the mean of the principal curvatures as in the current work, Gaussian curvature, etc. (See Pienaar⁴⁵ for an in-depth review). Given the larger number of regions with significant sulcal depth decrease in the very preterm group, immature sulci may still be driving increased curvature. Shallower sulci are missing sulcal wall area (low curvature), but have the same amount of sulcal trough area (high curvature), which results in higher average curvature in that local region¹⁴. The negative relationship between 1) sulcal depth and curvature and 2) gyrification index and curvature reinforces the idea that decreased folding may increase curvature in the very preterm group.

Our preterm only regression analyses confirmed BPD and ROP as clinical risk factors of abnormal cortical maturation in very preterm infants. A significant relationship persisted after controlling the final multivariable models for carefully selected clinical covariates. The negative relationship between BPD and surface area was

widespread, involving all lobes of the brain (Table 4). Our lobar analysis also revealed that parietal lobe sulcal depth was the main driver of the negative relationship between this cortical metric and ROP (Table 5). Although BPD is a well-established, independent risk factor for NDI, no structural abnormalities except ventriculomegaly consistently explain the poor outcomes associated with BPD^{27,46}. BPD and ROP both predicted NDI independently of structural injury in a large cohort of extremely preterm infants²¹, but our study is the first to link both to cortical maturational abnormalities. A few studies linked these antecedents to decreased white matter maturation, but none using the objective MRI measures of our study. Both BPD and ROP were associated in univariable analyses with lower overall maturation score (evaluated visually/qualitatively) on TEA MRI in preterm infants⁴⁷, but only BPD remained significant in multivariable analyses. Both BPD and ROP share systemic inflammation and hyperoxia as common mechanisms that could disrupt brain development. It is challenging to determine whether the link between BPD/ROP and cortical dysmaturation is causal or a result of the most developmentally delayed infants requiring more intervention and support. However, in a rat pup model, hyperoxia caused BPD-like lung changes, ROP-like hypervascularization, and reduced brain surface area⁴⁸, suggesting that BPD and ROP are interrelated and cause brain changes beyond those induced by prematurity. More work is needed to confirm similar causal effects in preterm infants.

Our study's strengths include a population-based cohort, assessment of quantitative cortical maturation measurements, and many covariates collected and temporally examined. However, several limitations should be acknowledged. Despite the large number of possible covariates collected, residual confounding could have introduced bias. Nevertheless, the association we identified with BPD and cortical surface area was especially strong. Furthermore, because we assessed numerous metrics, some false discovery is inevitable, even after applying FDR correction. Given that we excluded severely brain injured subjects, including those with ventriculomegaly, the brain changes reported here may be less severe than in other brain injured preterm cohorts. Finally, any automated segmentation is inherently imperfect. The dHCP pipeline represents a substantial improvement over labor-intensive manual segmentation, however its creators acknowledge a 2% rate of significant error³².

We identified widespread cortical maturation abnormalities at TEA in very preterm infants compared to full-term infants. These cortical abnormalities, specifically surface area and sulcal depth, appear to be exacerbated by clinical risk factors, BPD and ROP, respectively. Larger studies are needed to validate the relationship of these antecedents with cortical dysmaturation. Further work should examine the predictive value of cortical dysmaturation for NDI in VPT infants. This will allow clinicians to assess risk of impairment early and provide targeted early interventions.

Data availability

The datasets generated during the current study are available from the corresponding author on reasonable request.

Received: 2 August 2019; Accepted: 3 December 2019;

Published: 23 December 2019

References

- Chawanpaiboon, S. *et al.* Global, regional, and national estimates of levels of preterm birth in 2014: a systematic review and modelling analysis. *Lancet Glob. Heal.*, [https://doi.org/10.1016/S2214-109X\(18\)30451-0](https://doi.org/10.1016/S2214-109X(18)30451-0) (2019).
- Woodward, L. J., Edgin, J. O., Thompson, D. & Inder, T. E. Object working memory deficits predicted by early brain injury and development in the preterm infant. *Brain*, <https://doi.org/10.1093/brain/awh618> (2005).
- Johnson, S. Cognitive and behavioural outcomes following very preterm birth. *Semin. Fetal Neonatal Med.*, <https://doi.org/10.1016/j.siny.2007.05.004> (2007).
- Johnson, S. & Marlow, N. Preterm birth and childhood psychiatric disorders. *Pediatr. Res.*, <https://doi.org/10.1203/PDR.0b013e318212faa0> (2011).
- Vincer, M. J. *et al.* Increasing prevalence of cerebral palsy among very preterm infants: a population-based study. *Pediatrics*, <https://doi.org/10.1542/peds.2006-1522> (2006).
- van't Hof, J. *et al.* Predicting developmental outcomes in premature infants by term equivalent MRI: Systematic review and meta-analysis. *Syst. Rev.*, <https://doi.org/10.1186/s13643-015-0058-7> (2015).
- Hintz, S. *et al.* Neuroimaging and neurodevelopmental outcome in extremely preterm infants. *Pediatrics*, <https://doi.org/10.1542/peds.2014-0898> (2015).
- Parikh, N. A. Advanced neuroimaging and its role in predicting neurodevelopmental outcomes in very preterm infants. *Seminars in Perinatology*, <https://doi.org/10.1053/j.semperi.2016.09.005> (2016).
- Kapellou, O. *et al.* Abnormal cortical development after premature birth shown by altered allometric scaling of brain growth. *PLoS Med.*, <https://doi.org/10.1371/journal.pmed.0030265> (2006).
- Rathbone, R. *et al.* Perinatal cortical growth and childhood neurocognitive abilities. *Neurology*, <https://doi.org/10.1212/WNL.0b013e318233b215> (2011).
- Sølsnes, A. E. *et al.* Cortical morphometry and IQ in VLBW children without cerebral palsy born in 2003-2007. *NeuroImage Clin.*, <https://doi.org/10.1016/j.nicl.2015.04.004> (2015).
- Sripada, K. *et al.* Trajectories of brain development in school-age children born preterm with very low birth weight. *Sci. Rep.* **8**, 1-14 (2018).
- Engelhardt, E. *et al.* Regional impairments of cortical folding in premature infants. *Ann. Neurol.*, <https://doi.org/10.1002/ana.24313> (2015).
- Shimony, J. S. *et al.* Comparison of cortical folding measures for evaluation of developing human brain. *Neuroimage*, <https://doi.org/10.1016/j.neuroimage.2015.11.001> (2016).
- Zhang, Y. *et al.* Cortical structural abnormalities in very preterm children at 7 years of age. *Neuroimage*, <https://doi.org/10.1016/j.neuroimage.2015.01.005> (2015).
- Makropoulos, A. *et al.* Regional growth and atlas of the developing human brain. *Neuroimage*, <https://doi.org/10.1016/j.neuroimage.2015.10.047> (2016).
- Garcia, K. E. *et al.* Dynamic patterns of cortical expansion during folding of the preterm human brain. *Proc. Natl. Acad. Sci. USA*, <https://doi.org/10.1073/pnas.1715451115> (2018).

18. Bouyssi-Kobar, M. *et al.* Third Trimester Brain Growth in Preterm Infants Compared with in Utero Healthy Fetuses. *Obstetrical and Gynecological Survey*, <https://doi.org/10.1097/01.ogx.0000513225.92648.a4> (2017).
19. Dubois, J. *et al.* Primary cortical folding in the human newborn: An early marker of later functional development. *Brain*, <https://doi.org/10.1093/brain/awn137> (2008).
20. Davidson, L. & Berkelhamer, S. Bronchopulmonary Dysplasia: Chronic Lung Disease of Infancy and Long-Term Pulmonary Outcomes. *J. Clin. Med.*, <https://doi.org/10.3390/jcm6010004> (2017).
21. Van Marter, L. J. *et al.* Does bronchopulmonary dysplasia contribute to the occurrence of cerebral palsy among infants born before 28 weeks of gestation? *Arch. Dis. Child. Fetal Neonatal Ed.*, <https://doi.org/10.1136/adc.2010.183012> (2011).
22. Singer, L. T. *et al.* Preschool Language Outcomes of Children With History of Bronchopulmonary Dysplasia and Very Low Birth Weight. *J. Dev. Behav. Pediatr.*, <https://doi.org/10.1097/00004703-200102000-00003> (2001).
23. Short, E. J. *et al.* Cognitive and Academic Consequences of Bronchopulmonary Dysplasia and Very Low Birth Weight: 8-Year-Old Outcomes. *Pediatr.*, <https://doi.org/10.1542/peds.112.5.e359> (2003).
24. Natarajan, G. *et al.* Outcomes of extremely low birth weight infants with bronchopulmonary dysplasia: Impact of the physiologic definition. *Early Hum. Dev.*, <https://doi.org/10.1016/j.earlhumdev.2011.12.013> (2012).
25. Singer, L., Yamashita, T., Lilien, L., Collin, M. & Baley, J. A longitudinal study of developmental outcome of infants with bronchopulmonary dysplasia and very low birth weight. *Pediatrics* (1997).
26. Majnemer, A. *et al.* Severe bronchopulmonary dysplasia increases risk for later neurological and motor sequelae in preterm survivors. *Dev. Med. Child Neurol.*, <https://doi.org/10.1111/j.1469-8749.2000.tb00025.x> (2000).
27. Schmidt, B. *et al.* Impact of Bronchopulmonary Dysplasia, Brain Injury, and Severe Retinopathy on the Outcome of Extremely Low-Birth-Weight Infants at 18 Months. *JAMA* (2003).
28. Morken, T. S., Dammann, O., Skranes, J. & Austeng, D. Retinopathy of prematurity, visual and neurodevelopmental outcome, and imaging of the central nervous system. *Seminars in Perinatology*, <https://doi.org/10.1053/j.semperi.2019.05.012> (2019).
29. Glass, T. J. A. *et al.* Severe retinopathy of prematurity predicts delayed white matter maturation and poorer neurodevelopment. *Arch. Dis. Child. Fetal Neonatal Ed.*, <https://doi.org/10.1136/archdischild-2016-312533> (2017).
30. Molloy, C. S., Anderson, P. J., Anderson, V. A. & Doyle, L. W. The long-term outcome of extremely preterm (<28 weeks' gestational age) infants with and without severe retinopathy of prematurity. *J. Neuropsychol.* **10**, 276–294 (2016).
31. Schmidt, B. *et al.* Prediction of Late Death or Disability at Age 5 Years Using a Count of 3 Neonatal Morbidities in Very Low Birth Weight Infants. *J. Pediatr.*, <https://doi.org/10.1016/j.jpeds.2015.07.067> (2015).
32. Makropoulos, A. *et al.* The developing human connectome project: A minimal processing pipeline for neonatal cortical surface reconstruction. *Neuroimage*, <https://doi.org/10.1016/j.neuroimage.2018.01.054> (2018).
33. Gousias, I. S. *et al.* Magnetic Resonance Imaging of the Newborn Brain: Automatic Segmentation of Brain Images into 50 Anatomical Regions. *PLoS One*, <https://doi.org/10.1371/journal.pone.0059990> (2013).
34. Yeo, I. N. K. & Johnson, R. A. A new family of power transformations to improve normality or symmetry. *Biometrika*, <https://doi.org/10.1093/biomet/87.4.954> (2000).
35. Maalouf, E. F. *et al.* Magnetic resonance imaging of the brain in a cohort of extremely preterm infants. *J. Pediatr.*, [https://doi.org/10.1016/S0022-3476\(99\)70133-2](https://doi.org/10.1016/S0022-3476(99)70133-2) (1999).
36. Peterson, B. S. *et al.* Regional Brain Volumes and Their Later Neurodevelopmental Correlates in Term and Preterm Infants. *Pediatrics* (2003).
37. Parikh, N. A., Lasky, R. E., Kennedy, K. A., McDavid, G. & Tyson, J. E. Perinatal Factors and Regional Brain Volume Abnormalities at Term in a Cohort of Extremely Low Birth Weight Infants. *PLoS One*, <https://doi.org/10.1371/journal.pone.0062804> (2013).
38. Bancalari E, J. A. NICHD/NHLBI/ORD Workshop Summary - Bronchopulmonary Dysplasia. *Am. J. Respir. Crit. Care Med.*, <https://doi.org/10.1164/ajrccm.163.7.2011060> (2001).
39. International Committee for the Classification of Retinopathy of Prematurity. The International Classification of Retinopathy of Prematurity revisited. *Arch. Ophthalmol. (Chicago, Ill. 1960)* **123**, 991–9 (2005).
40. Nelson, K. B. & Ellenberg, J. H. Antecedents of Cerebral Palsy: I. Univariate Analysis of Risks. *Am. J. Dis. Child.*, <https://doi.org/10.1001/archpedi.1985.02140120077032> (1985).
41. Leviton, A. Preterm Birth and Cerebral Palsy: Is Tumor Necrosis Factor the Missing Link? *Dev. Med. Child Neurol.*, <https://doi.org/10.1111/j.1469-8749.1993.tb11688.x> (2008).
42. Mickey, R. M. & Greenland, S. The impact of confounder selection criteria on effect estimation. *Am. J. Epidemiol.*, <https://doi.org/10.1093/oxfordjournals.aje.a115101> (1989).
43. Kidokoro, H., Neil, J. J. & Inder, T. E. New MR imaging assessment tool to define brain abnormalities in very preterm infants at term. *Am. J. Neuroradiol.*, <https://doi.org/10.3174/ajnr.A3521> (2013).
44. Slaughter, L. A., Bonfante-Mejia, E., Hintz, S. R., Dvorchik, I. & Parikh, N. A. Early conventional MRI for prediction of neurodevelopmental impairment in extremely-low-birth-weight infants. *Neonatology*, <https://doi.org/10.1159/000444179> (2016).
45. Pienaar, R., Fischl, B., Caviness, V., Makris, N. & Grant, P. E. A methodology for analyzing curvature in the developing brain from preterm to adult. *Int. J. Imaging Syst. Technol.*, <https://doi.org/10.1002/ima.20138> (2008).
46. Anderson, P. J. & Doyle, L. W. Neurodevelopmental Outcome of Bronchopulmonary Dysplasia. *Seminars in Perinatology*, <https://doi.org/10.1053/j.semperi.2006.05.010> (2006).
47. Neubauer, V., Junker, D., Griesmaier, E., Schocke, M. & Kiechl-Kohlendorfer, U. Bronchopulmonary dysplasia is associated with delayed structural brain maturation in preterm infants. *Neonatology*, <https://doi.org/10.1159/000369199> (2015).
48. Poon, A. W. *et al.* Impact of bronchopulmonary dysplasia on brain and retina. *Biol. Open* (2016).

Acknowledgements

National Institutes of Health grants R01-NS094200 and R01-NS096037 supported this study. The funders played no role in the design, analysis, or presentation of findings. We thank Jennifer Notestine and Valerie Marburger for study coordination, Josh Goldberg for recruitment assistance, Jonathan Dudley for coding help, Mark Smith for serving as our lead MR technologist, and the families and NICU personnel that made this study possible.

Author contributions

N.A.P. designed this study. N.A.P. and L.H. collected the data. J.E.K., M.A., V.S.P.I. and N.A.P. analyzed the data. J.E.K. wrote the manuscript. J.E.K., V.S.P.I., L.H., M.A. and N.A.P. reviewed and edited the manuscript. All authors take full responsibility for the research contained in this article.

Competing interests

The authors declare no competing interests.

Additional information

Supplementary information is available for this paper at <https://doi.org/10.1038/s41598-019-56298-x>.

Correspondence and requests for materials should be addressed to N.A.P.

Reprints and permissions information is available at www.nature.com/reprints.

Publisher's note Springer Nature remains neutral with regard to jurisdictional claims in published maps and institutional affiliations.



Open Access This article is licensed under a Creative Commons Attribution 4.0 International License, which permits use, sharing, adaptation, distribution and reproduction in any medium or format, as long as you give appropriate credit to the original author(s) and the source, provide a link to the Creative Commons license, and indicate if changes were made. The images or other third party material in this article are included in the article's Creative Commons license, unless indicated otherwise in a credit line to the material. If material is not included in the article's Creative Commons license and your intended use is not permitted by statutory regulation or exceeds the permitted use, you will need to obtain permission directly from the copyright holder. To view a copy of this license, visit <http://creativecommons.org/licenses/by/4.0/>.

© The Author(s) 2019, corrected publication 2021